Density predictions using V_p and V_s sonic logs

Colin C. Potter and Robert R. Stewart

ABSTRACT

We use *P*-wave, V_p, and *S*-wave, V_s, velocity logs to predict density, ρ, values. In particular, Gardner's and Lindseth's empirical relationships are used to estimate the coefficients for *P*-wave and *S*-wave data and to investigate the relationship between *P*-wave and *S*-wave velocities and bulk densities. The data is from four wells in the Blackfoot field and one in the Chin Coulee area of Alberta. The *S*-wave velocities give a good approximation to Gardner's relationship and we find that ρ=0.37$V_s^{0.22}$. The variance or scatter about the best-fit line for predicting densities for both Gardner's and Lindseth's relationship is better for *S*-wave than *P*-wave velocities. We suggest there is a relation between *S*-wave impedance and density and that *S*-wave velocity can be used to predict density.

INTRODUCTION

The prediction of density is a major goal in petroleum exploration. Seismically speaking, we thus need to find a relationship between velocities and rock densities. Density prediction using both *P*-wave and *S*-wave velocities might improve, if both velocities are related to density. We investigate the relationship between *S*-wave velocity and density for a better understanding of petrophysics, inversion, and *S*-wave velocity as a lithology/porosity indicator.

There are many empirical relationships that describe *P*-wave velocity as a function of density, but very few that compare *S*-wave velocities with densities. Birch (1961) gave the fundamental empirical relation:

$$V_p = a + b\rho \tag{1}$$

where a and b are empirical parameters and V_p is in km/s and ρ is in g/cm^3, which is the basis for many other linear regression analyses. Further empirical relations found that the mineral composition of most rocks affect both velocity and density in the same direction giving a correlation between them.

Gardner et al. (1974) conducted a series of controlled field and laboratory measurements of saturated sedimentary rocks and determined a relationship between *P*-wave velocity and density that has long been used in seismic analysis:

$$\rho = aV^b \tag{2}$$

where ρ is in g/cm^3, a is 0.31 when V is in m/s and is 0.23 when V is in ft/s and b is 0.25 (Figure 1). Major sedimentary rocks generally define a narrow corridor around this prediction. The major deviations from this trend are coals and evaporites. Since V_p and V_s show lithology discrimination, these can be useful for predicting density.

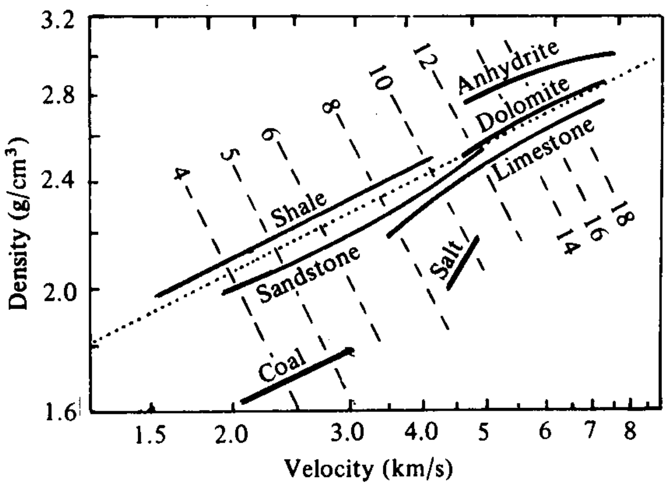

Figure 1. Density versus *P*-wave velocity (log-log scale). Gardner's empirical relationship where the dotted line pertains to equation (2) (from Sheriff and Geldart, 1995).

Lindseth (1979) used Gardner's empirical data to derive the following relationship between acoustic impedance and velocity:

$$\rho V=(V-c)/d \tag{3}$$

where ρ is in g/cm^3, V is in ft/s, c is 3460 and d is 0.308 (Figure 2). Lindseth's results found that detailed velocity measurements could be used to predict rock type.

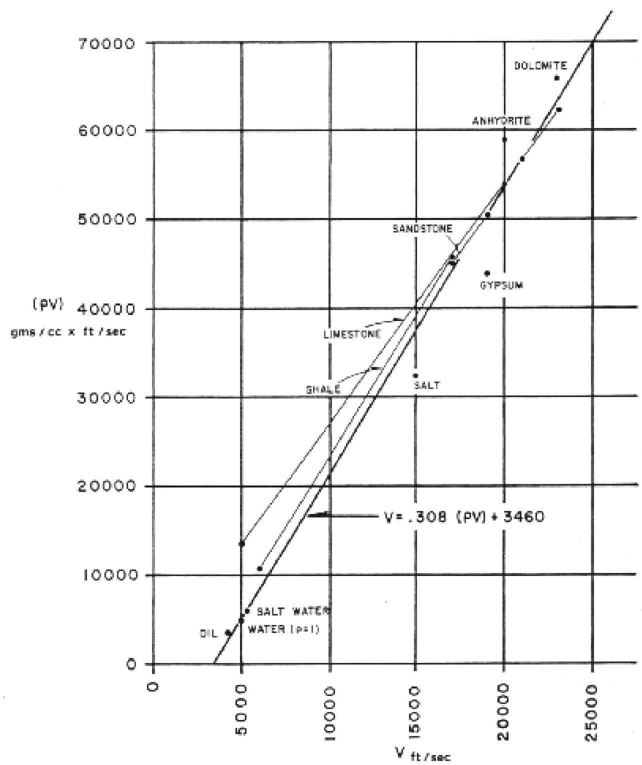

Figure 2. Values of acoustic impedance versus rock velocity. Lindseth's empirical relationship where the thick line pertains to equation (3).

This paper investigates the use of Gardner's relationship and Lindseth's relationship with both *P*-wave and *S*-wave velocities to predict density. The log data studied in this report are primarily taken from the 08-08, 04-16, 12-16, and 09-17 wells within the Blackfoot field located near Strathmore, Alberta. The Glauconitic member of the lower Cretaceous is of particular interest here. Within it are a shale-filled channel and a porous sand-filled channel. The sand-filled channel is the producing unit in this area. Other log data used is from the 03-21 well from the Chin Coulee region in Southern Alberta for comparison to the Blackfoot wells.

We are interested in determining whether density estimation can be improved by V_p and V_s, and how *S*-wave impedance is related to *S*-wave velocity.

METHODS

The wells used in this paper were selected because they have dipole sonic logs, which are mainly over the zone of interest. The density logs used are bulk densities. The MATLAB scientific programming environment was used to obtain the cross-plots, diagrams, estimated coefficients, and statistics. We use V_p and V_s in Gardner's and Lindseth's relationships to predict density and the corresponding variables. A polynomial that best fits the data in a least-squares sense is applied to these relationships to estimate the coefficients *a*, *b*, *c* and *d*. For Gardner's coefficients, *a* and *b*, a program in MATLAB called gardnerexp (from CREWES seismic toolbox) calculates the best fit polynomial for density versus velocity plots and then the coefficients (Figures 4,5, & 10). It also plots the normalized logs of velocity on the left and density on the right. By writing equation (2) in a log-log sense, a linear equation is obtained where log(*a*) is the intercept and *b* is the slope of the best-fit line. This is shown by the following equation:

$$\log(\rho)=b*\log(V)+\log(a) \qquad (4)$$

where log(*a*) is converted back to *a*. In the same sense, Lindseth's relationship equation (3) can be arranged to obtain the linear equation:

$$\rho=1/d-c/(dV) \quad \text{or} \quad \rho=3.25-11233V^{-1} \qquad (5)$$

where $1/d$ or 3.25 is the intercept and c/d or 11233 is the slope of the line. The intercepts and slopes of the best-fit lines are then converted back to *c* and *d*. To comply with Lindseth's empirical linear relationship, all density values are in g/cm^3 and velocity values in ft/s.

The MATLAB function 'polyfit' was used to find the coefficients of the polynomials that best fits the data in a least squares sense. The 'polyval' function evaluates the polynomial at all points of X. Then, the functions 'std' and 'cov' were used to calculate the standard deviation and the variance, respectively. The variance evaluates the amount of scatter about the best-fit line. Since the 'std' function normalizes the data by (n-1) and the data is a normal distribution, 'cov' gives the best unbiased estimate of the variance. The estimated coefficients and the corresponding variances are shown in Tables 1 and 2.

RESULTS

Velocity log data from the Blackfoot field are cross-plotted in Figure 3. A quasi-linear relation between V_s and V_p is in evidence.

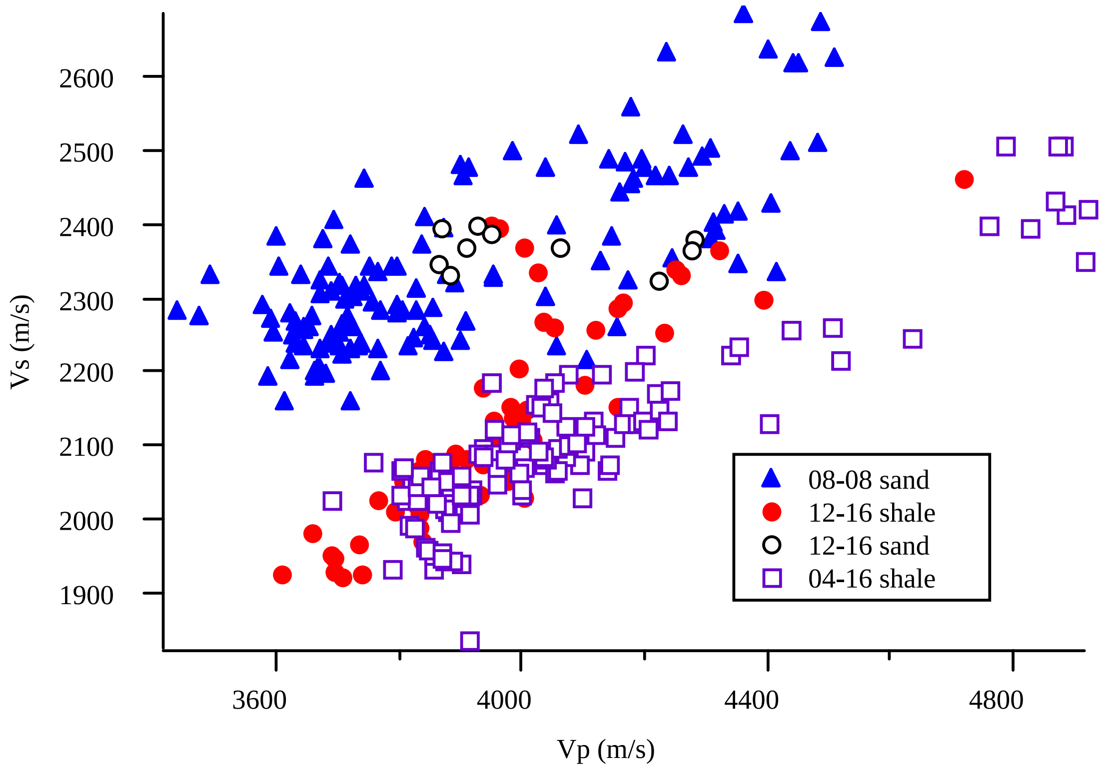

Figure 3. V_s versus V_p in the Glauconitic Formation for the 08-08, 04-16, and 12-16 wells (from Potter et al., 1996).

Figures 4, 5, and 6 are density versus velocity plots for the 09-17 well from the top of the Mannville to the Mississippian showing the best-fit line through the data. The MATLAB program 'gardnerexp' executes Gardner's coefficients. The density-V_p plot give results of 0.208 for *a* and 0.264 for *b*, while the density-V_s plots give results of 0.214 and 0.280, respectively. These figures are well in the range of Gardner's coefficients. Figure 6 is a log-log plot of density versus V_p and V_s that shows the linear polynomial for the best-fit lines. This is the visual representation for equation (4) where the coefficients could be extrapolated and it shows the amount of scatter about the line.

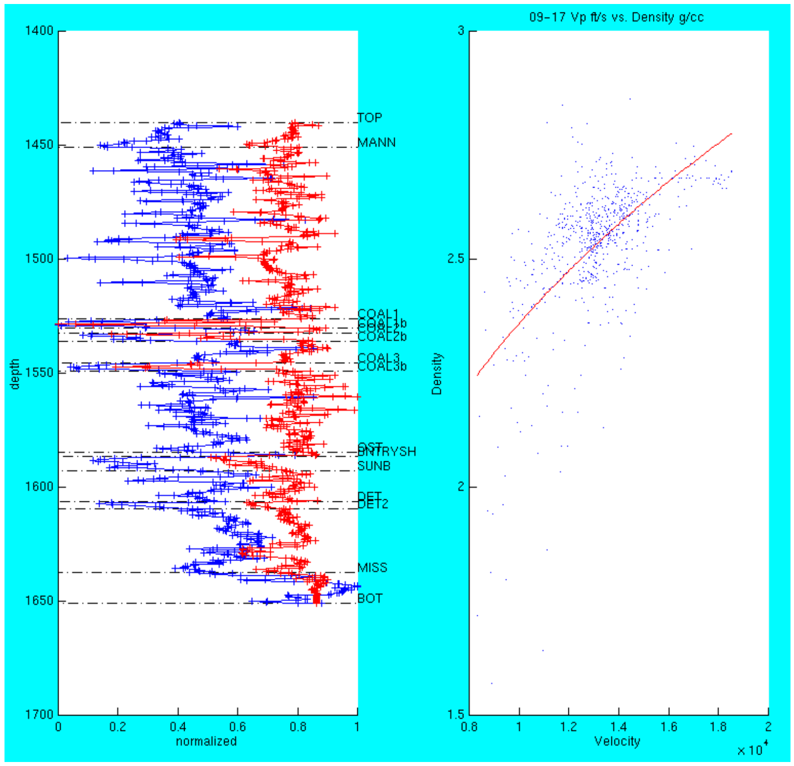

Figure 4. Density (g/cm3) versus V_p (ft/s) for 09-17 well showing the best-fit line through the data. The V_p log is on the right and density on the left.

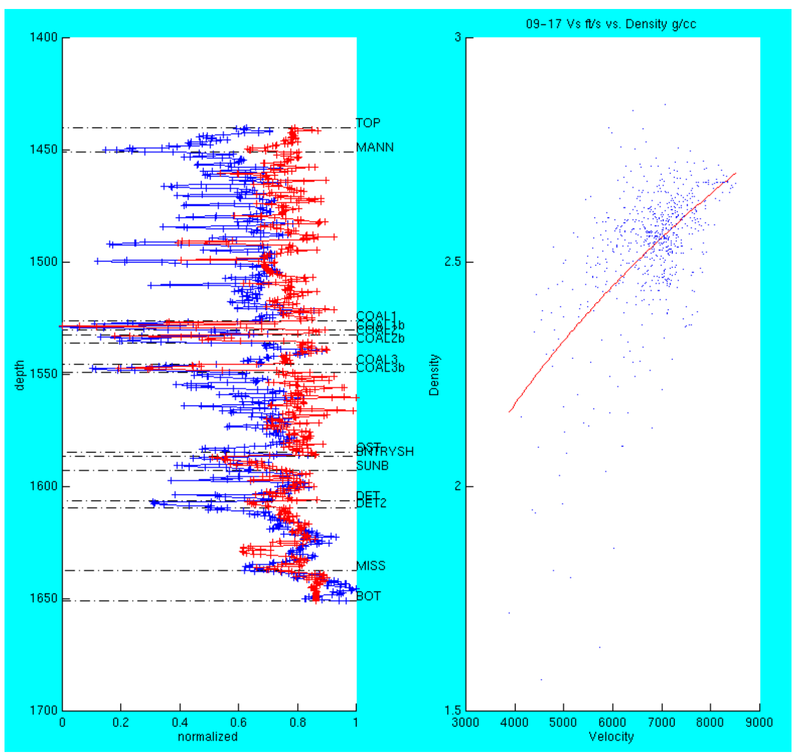

Figure 5. Density (g/cm3) versus V_s (ft/s) for 09-17 well showing the best-fit line through the data. The V_s log is on the right and the density on the left.

Contents

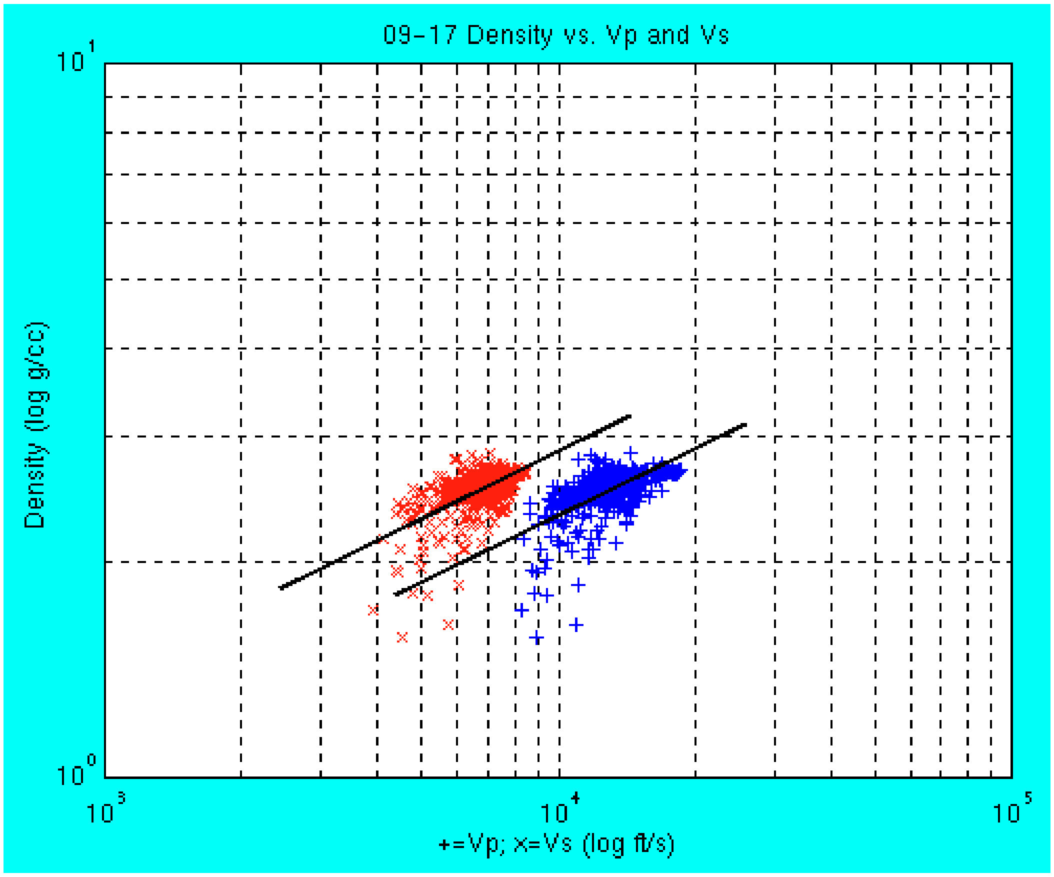

Figure 6. Density versus V_p and V_s log-log plot for 09-17 well showing the best-fit lines through the data. This plot is used for Gardner's relationship and is the visual representation for equation (4).

Figures 7, 8, and 9 are density versus reciprocal velocity plots for the 09-17 well from the top of the Mannville to the Mississippian that represents Lindseth's relationship and equation (5). Figures 8 and 9 are three way cross-plots of Figure 7. These are for visual representation only. The density-1/V_p plot gives results of 2509 for *c* and 0.315 for *d*, while the density-1/V_s plot give results of 1278 and 0.317, respectively. The coefficients for the V_p data are relatively close to that of Lindseth's, while the V_s data coefficients are not. This is quite understandable since Lindseth's work involved *P*-wave data only.

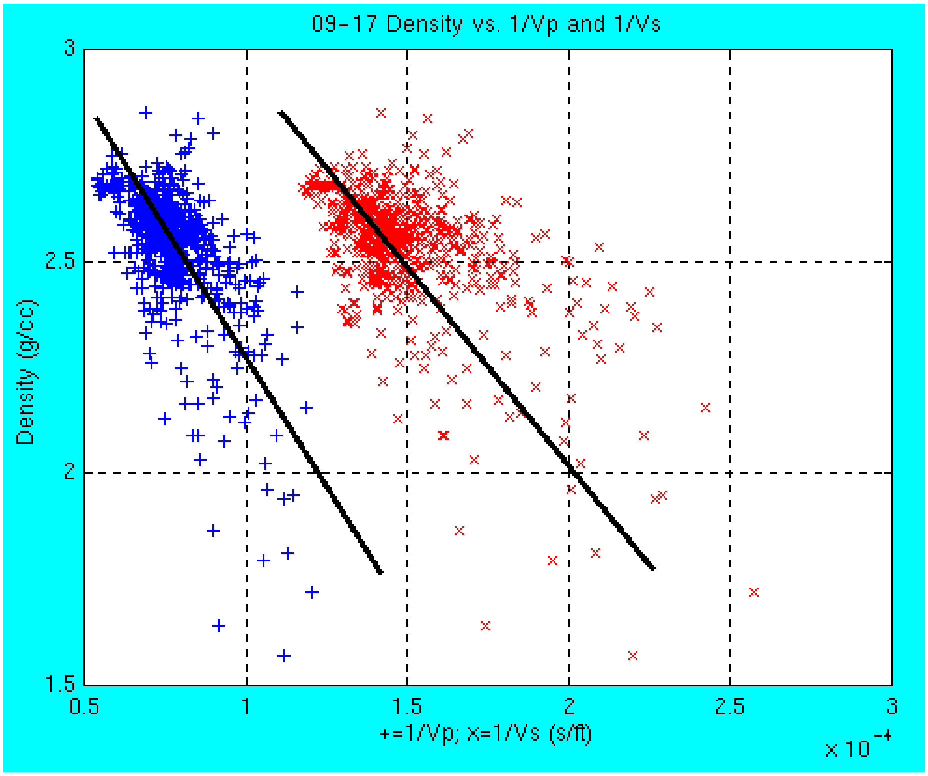

Figure 7. Density versus $1/V_p$ and $1/V_s$ for 09-17 well. This plot is used for Lindseth's relationship and is the visual representation for equation (5).

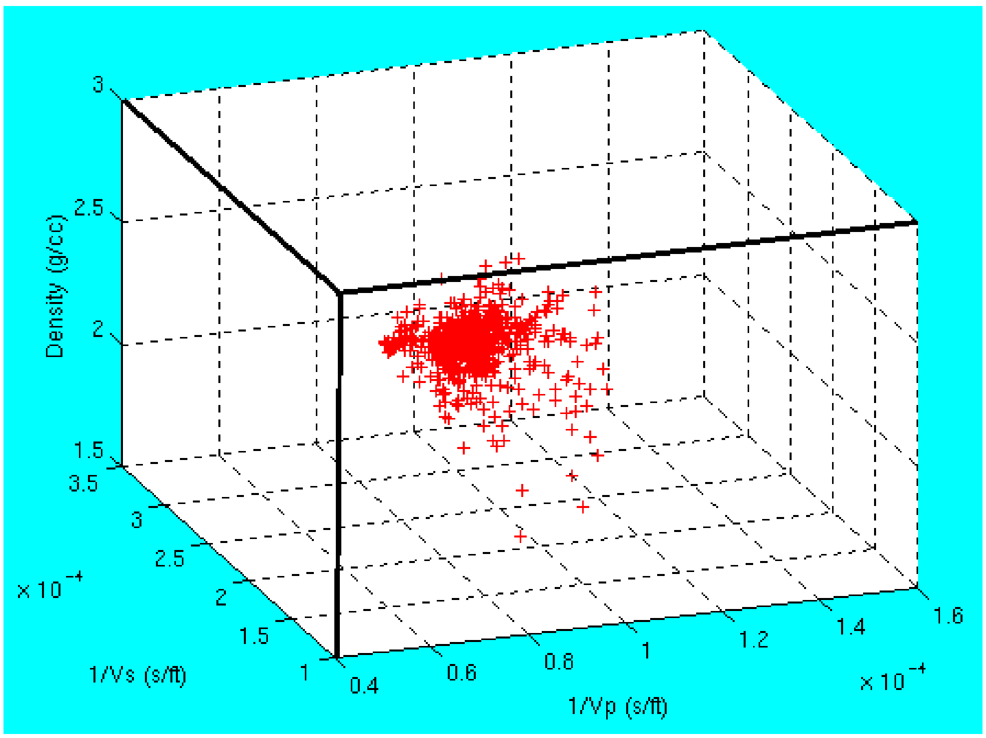

Figure 8. Density versus $1/V_p$ versus $1/V_s$ for 09-17 well showing the relation for Lindseth's relationship.

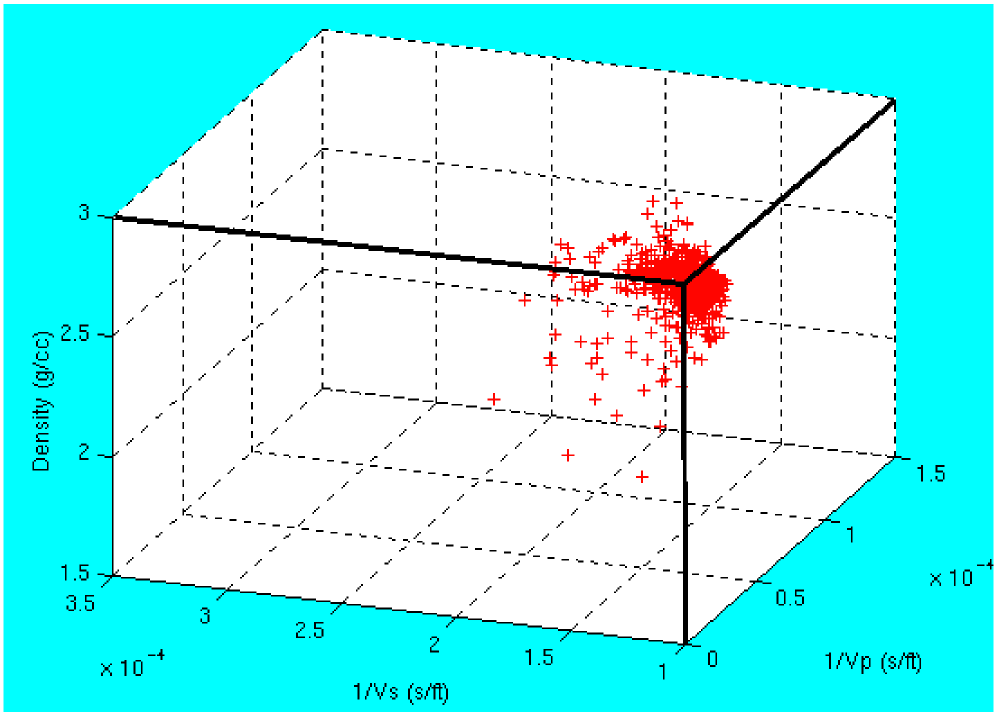

Figure 9. Density versus 1/V_s versus 1/V_p for 09-17 well showing the relation for Lindseth's relationship.

Table 1 shows the results for the 12-16, 09-17, and 08-08 wells. These three wells are grouped together, since dipole sonics are relatively over the same interval. Note that the results for the coefficients of V_p fall within Gardner's and Lindseth's values, while the V_s coefficients are less accurate. Of course, Gardner and Lindseth both used compressional wave velocities in their experiments and not shear wave velocities.

Well Name	12-16		09-17		08-08	
Velocity	V_p	V_s	V_p	V_s	V_p	V_s
a $\rho = aV^b$	0.238	0.370	0.208	0.214	0.190	0.371
b	0.249	0.218	0.264	0.280	0.271	0.214
Gardner's Variance	0.0014	0.0015	0.0013	0.0012	0.0020	0.0012
c $\rho V = (V-c)/d$	2646	1089	2509	1278	2991	1183
d	0.313	0.323	0.313	0.313	0.313	0.333
Lindseth's Variance	0.0091	0.0094	0.0078	0.0067	0.0129	0.0070

Table 1. Summary of coefficients and statistical analysis for density models using V_p and V_s (ft/s) for 12-16, 09-17, and 08-08 wells.

The 04-16 well and all four wells combined results are in Table 2. The first two columns of results are for the formation interval from above the top of the Second White Speckled Shale to the Mississippian. The second two columns are from the

Viking to the Mississippian (i.e. 04-16 Viking). The second set results show much better correlation of coefficients than that of the first set. The densities above the Viking are approximately the same as the densities from the Viking to the Mannville, in contrast to the velocities, which are much lower above the Viking (Figure 10). The results from all four wells combined are very good. The coefficients resemble those of Gardner's and Lindseth's closely. The main point is the comparison of the variances between the V_p and V_s data. In all cases, except the 12-16 well, the variances for the V_s data are smaller than those of the V_p data.

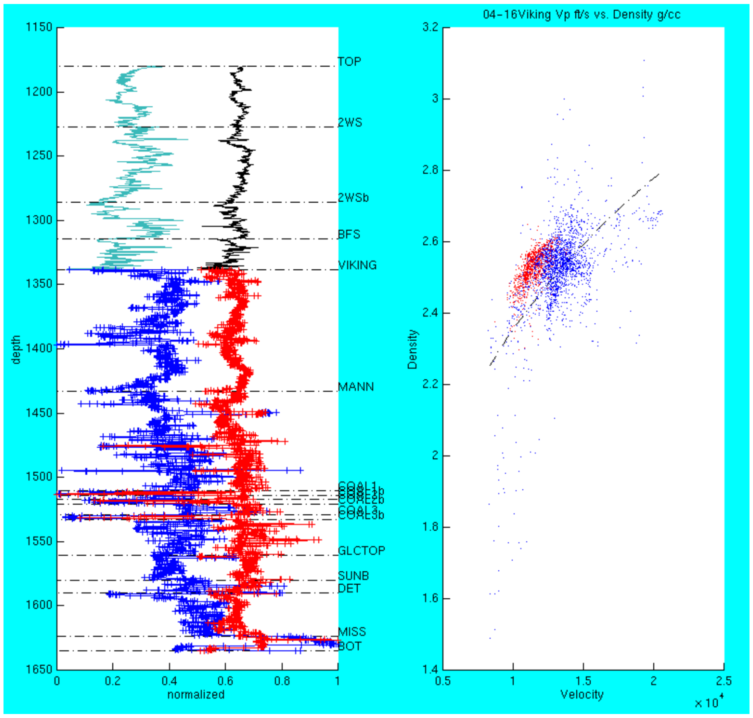

Figure 10. Density (g/cm[3]) versus V_p (ft/s) for 04-16 well from Viking to Bottom showing the best-fit line through the data. Note the lower velocities (left log) above the Viking as compared to below the Viking in contrast to the similar densities (right log) above and below the Viking.

Well Name	04-16		04-16 Viking		Four Wells	
Velocity	V_p	V_s	V_p	V_s	V_p	V_s
a $\rho=aV^b$	0.554	0.808	0.266	0.507	0.226	0.366
b	0.161	0.130	0.237	0.181	0.255	0.238
Gardner's Variance	0.0005	0.0004	0.0010	0.0009	0.0014	0.0012
c $\rho V=(V-c)/d$	1583	1089	2322	881	2617	1108
d	0.345	0.357	0.323	0.345	0.316	0.329
Lindseth's Variance	0.0029	0.0028	0.0060	0.0053	0.0090	0.0071

Table 2. Summary of coefficients and statistical analysis for density models using V_p and V_s (ft/s) for 04-16, 04-16 Viking, and all four wells.

The Chin Coulee 03-12 well has dipole data from 280m to 960m. Although the coefficients for this well did not match those of Gardner's and Lindseth's well, the variances were still better for V_s data.

We find that standard deviation and variance are smaller for V_s than for V_p in these density models for four of the five wells analyzed. We also find an empirical relationship similar to that of Gardner's for V_s from the results. From equation (2), we find that

$$\rho = 0.37 V_s^{0.22} \tag{6}$$

where the coefficients were estimated from the results and from replicating Gardner's relationship with a series of *P*-wave velocities, then best-fitting V_s data to the original equation. However, this is inconclusive for V_s less than 5000ft/s and should be used with care. Further testing of this hypothesis with additional well logs is required.

CONCLUSIONS

Although Gardner's and Lindseth's relationship were originally developed with *P*-wave data, we find that in Gardner's case V_s fits the expected exponent for density predictions well and that the coefficient for *a* is about 0.37. We suggest that V_s can be used to predict density and there is a relationship between *S*-wave impedance and velocity. For four of five wells investigated, V_s has smaller standard deviations and variances in Gardner’s and Lindseth’s relationships than does V_p.

ACKNOWLEDGEMENTS

We would like to thank PanCanadian Petroleum Limited for the data and the CREWES sponsors for their support. We would also like to thank Ayon K. Dey for initial density prediction insight and related discussions.

REFERENCES

Birch, F., 1961, The velocity of compressional waves in rocks to 10 kilobars (Part II), Journ. Geophys. Res., 66, 2199-2224.

Gardner, G.H.F., Gardner, L.W., and Gregory, A.R., 1974, Formation velocity and density – The diagnostic basics for stratigraphic traps: Geophysics, 39, 770-780.

Lindseth, R.O., 1979, Synthetic sonic logs – a process for stratigraphic interpretation: Geophysics, 44, 3-26.

Potter, C.C., Miller, S.L.M., Margrave, G.F., 1996, Formation elastic parameters and synthetic P-P and P-S seismograms for the Blackfoot field: CREWES Research Report 1996, Ch 37.

Sheriff, R.E., and Geldart, L.P., 1995, Exploration Seismology, Second Edition: Cambridge University Press, New York, NY.